Electrocatalysts for Hydrogen Peroxide Reduction Used in Fuel Cells

Yusuke Yamada

Citation	Anion Exchange Membrane Fuel Cells. pp 141-168.
Issue Date	2018-03-22
Type	Book chapter
Textversion	author
Rights	This is accepted manuscript version of the book chapter in Anion Exchange Membrane Fuel Cells. After it is published, it will be found at: https://doi.org/10.1007/978-3-319-71371-7_5 This is not the published version. Please cite only the published version.
DOI	10.1007/978-3-319-71371-7_5

Self-Archiving by Author(s)
Placed on: Osaka City University

Electrocatalysts for Hydrogen Peroxide Reduction Used in Fuel Cells

Yusuke Yamada

Department of Applied Chemistry and Bioengineering, Graduate School of Engineering,
Osaka City University, 3-3-138 Sugimoto, Sumiyoshi, Osaka 558-8585, Japan
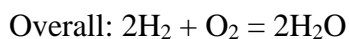*Tel & Fax: +81-6-6605-2693*
E-mail: ymd@a-chem.eng.osaka-cu.ac.jp

Introduction

Fuel cells technology has attracted much attention owing to their high conversion efficiency in chemical energy to electrical energy with simple structures, clean emissions, insignificant scale effect, etc. The theoretical conversion efficiency of a typical proton exchange membrane fuel cell operating H_2 and O_2 as a fuel and oxidant, respectively, reaches ~40%. Other than H_2/O_2 fuel cells, various types of organic chemicals including hydrocarbons, alcohols, aldehydes and hydrocarbons, are potential fuels for operating fuel cells. The open circuit voltage of a fuel cell is determined by difference between the reduction potential of an oxidant and oxidation potential of fuels.

Typically fuel cells are assembled by four components that are a cathode, an anode, an ion-exchange membrane, and an external circuit. Under the operation conditions, fuel compounds are oxidatively decomposed into protons, electrons and other products at the anode. The protons thus formed move to the cathode side passing through the ion-exchange membrane, and electrons passing through the external circuit to reduce oxygen to form water. Theoretical output potentials of fuel cells can be calculated from the standard electrode potentials of the reactions at the anode and cathode. The expected output potential of a typical H_2/O_2 fuel cell is 1.23 V based on the following potentials[1]:
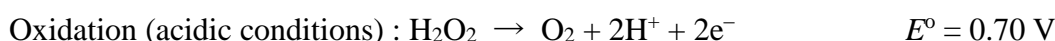
Anode: $2H_2 = 4H^+ + 4e^-$ $\qquad\qquad$ $E^o = 0.0$ V vs NHE $\qquad$ (1)

Cathode: $O_2 + 4H^+ + 4e^- = 2H_2O$ $\qquad$ $E^o = 1.23$ V vs NHE $\qquad$ (2)

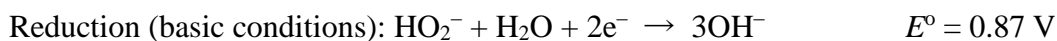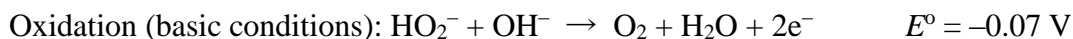Overall: $2H_2 + O_2 = 2H_2O$ $\qquad\qquad$ $E = 1.23$ V

The output potentials of other fuel cells such as methanol/O_2 and ethanol/O_2, were 1.21 and 1.18 V, respectively, which are lower than those of rechargeable batteries currently available in the market, such as lithium ion battery (~3 V) and lead battery (~2 V). Higher output potentials with high power density can be achieved by employing stronger oxidant in liquid or solid such as H_2O_2 instead of gaseous O_2 at the cathode sides, because the standard electrode potential of H_2O_2 reduction of 1.77 V ($H_2O_2 + 2H^+ + 2e^- = 2H_2O$; $E^o = 1.77$ V vs NHE) is that of O_2 (eq. 2; $E^o = 1.23$ V vs NHE), and the high density of 1.45 g cm^{-3} (23.4 cm^{-3} for 1 mol), which allows to assemble fuel cells with high power density.[2,3] Furthermore, H_2O_2 can be easily obtained by two-electron reduction of naturally abundant O_2 with various reductants including water.[3-8] A demerit of H_2O_2 is an explosive nature that caused by decomposition into water and oxygen by disproportionation, which is catalyzed by various metals and metal oxides. However, H_2O_2 can be stored safely even at high concentration by forming adducts with $NaHCO_3$ or urea in the solid state.[5] Thus, development in superior electrodes for H_2O_2 reduction is necessary to construct high power fuel cells. Various electrodes composed of metal, metal oxide and metal complexes have been investigated for electrochemical H_2O_2 reduction. In this review, electrocatalysts for H_2O_2 reduction used in fuel cells are categorized into three groups that are metal, metal oxide and complexes.

Review of Redox Properties of H_2O_2 under Acidic and Basic Conditions

The standard electrode potentials of H_2O_2 oxidation and reduction under acidic and basic conditions are as follows [1]:

Oxidation (acidic conditions) : $H_2O_2 \rightarrow O_2 + 2H^+ + 2e^-$ $\qquad\qquad$ $E^o = 0.70$ V

Reduction (acidic conditions) : $H_2O_2 + 2H^+ + 2e^- \rightarrow 2H_2O$ $\qquad\qquad$ $E^o = 1.76$ V

In basic solution, H_2O_2 forms deprotonated HO_2^-.

Oxidation (basic conditions): $HO_2^- + OH^- \rightarrow O_2 + H_2O + 2e^-$ $\quad\quad E^o = -0.07$ V

Reduction (basic conditions): $HO_2^- + H_2O + 2e^- \rightarrow 3OH^-$ $\quad\quad E^o = 0.87$ V

The reduction potential under acidic conditions is more positive than that under basic conditions by ca. 0.9 V, suggesting that H_2O_2 behaves as more powerful oxidant to provide high power voltage and power density. Additionally, H_2O_2 decomposition has been reported to be much slower under acidic conditions than basic conditions as predicted by the oxidation potentials under acidic and basic conditions. Based on these considerations, catholyte of fuel cells should contain H_2O_2 together with acids such as phosphoric acid or Lewis acid, metal ions, for both superior electron acceptability and stability to avoid decomposition by disproportionation.

H_2O_2 Reduction Catalysts Used in Fuel Cells

Metal Catalysts

a. Pt-Based Catalysts

In general, fuel cells require an electrolyte membrane to avoid thermal reaction of fuel and oxidant on electrodes. However, a fuel cell without membrane can be assembled by utilization of a microchannel reactor, because co-laminar flow is predominant in the microchannel. A H_2O_2/H_2O_2 fuel cell using a microchannel reactor configuration was constructed employing Pt electrodes for both anode and cathode as shown in Fig. 1A and 1B.[9] H_2O_2 can act as both fuel and oxidant, and reduction and oxidation of H_2O_2 are thermodynamically favorable under acidic and basic conditions, respectively. In the fuel cell, acidic H_2O_2 solution ($[H_2O_2]/[H_2SO_4] = 2$) and basic H_2O_2 solution ($[H_2O_2]/[NaOH] = 1$) were supplied to the Pt cathode and Pt anode, resulting in electrical power generation with the maximum power density of 23 mW cm^{-2} with the open circuit voltage of 700 mV (Fig. 1C).[9]
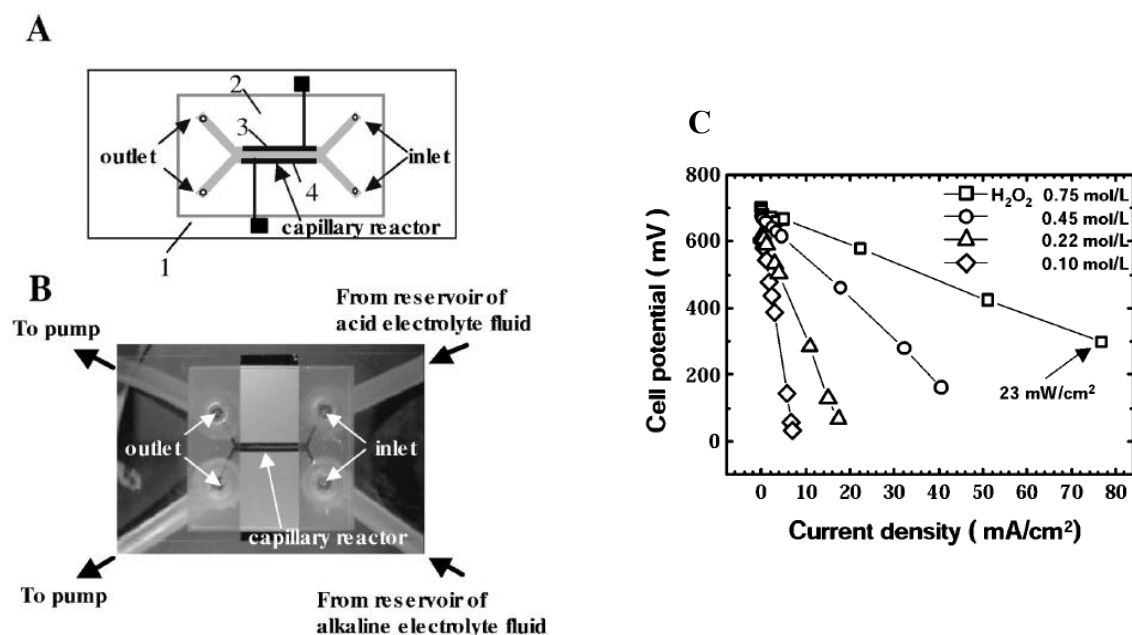
Fig. 1. (A) Schematic drawing and (B) photograph of the microchannel reactor of a H_2O_2/H_2O_2 fuel cell. The cell is a simple capillary reactor, where it consists of (1) glass slide and (2) cover glass and epoxy resin spacer (50 μm thick) between them. Pt electrodes (3) and (4) are placed on the capillary undersurface. Outside the photograph of (B) each inlet and outlet is connected to a fluid reservoir and flow pump, respectively. (C) Cell performance of the H_2O_2/H_2O_2 fuel cell at room temperature. At 0.75 M H_2O_2 (open squares), the maximum power density is 23 mW cm^{-2} with cell voltage of 300 mV and current density of 76 mA cm^{-2}.[9]

Such a microreactor configuration without membrane was also applied for constructing a formic acid/H_2O_2 fuel cell and a methanol/H_2O_2 fuel cell.[10,11] A microreator HCOOH/H_2O_2 fuel cell constructed with Pd electrodeposited on Au as the anode and a Pt/Pd cathode exhibited the maximum power density of 30 mW cm^{-2} under the optimized conditions where both anolyte and catholyte contained 2 M phosphate (Fig. 2).[10] The power density was similar to that achieved for a conventional two compartment HCOOH/H_2O_2 fuel cell using a polymer electrolyte membrane and Pt based catalysts for both anode and cathode.[12] A MeOH/H_2O_2 fuel cell with a microreactor configuration was constructed with ladder-shaped microchannels to

4

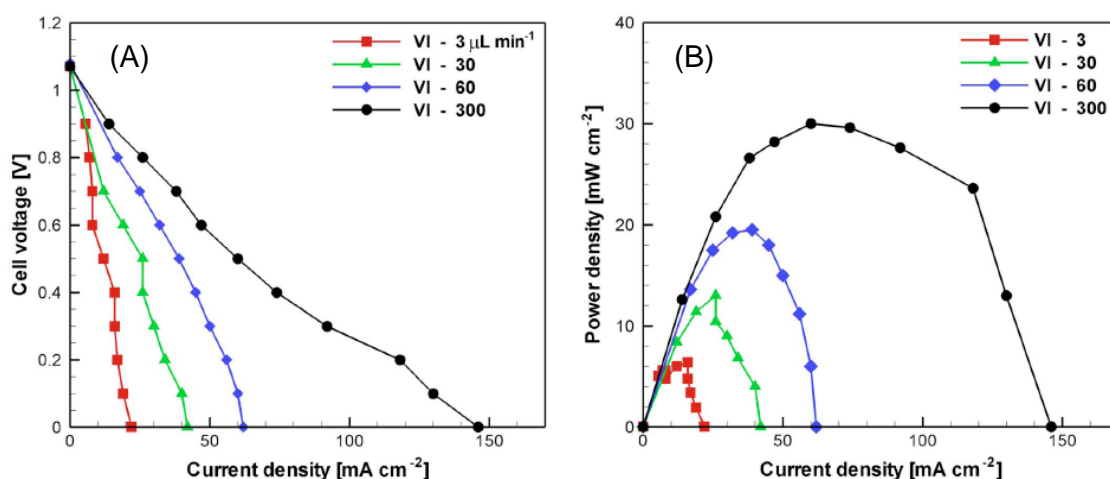**Fig. 2.** (A) Polarization and (B) power density curves obtained experimentally at flow rates ranging from 3 to 300 L min^{-1}. Fuel cell with Pt/Pd cathode (140/70 µm channel) was employed using standard solutions (1 M HCOOH in 2 M phosphate and 2 M H$_2$O$_2$ in 2 M phosphate). [10]

maintain co-laminar flow firmly (Fig. 3A). The fuel cell was fed with a mixture of 2 M CH$_3$OH and 0.5 M H$_2$SO$_4$ as anolyte and a mixture of 2 M H$_2$O$_2$ and 0.5 M H$_2$SO$_4$ as catholyte. The fuel cell with ladder-shaped channel exhibited high maximum power density of 12.24 mW cm^{-2} compared with a fuel cell with normal channel microreactor (Fig. 3B). [11] The power density achieved for the HCOOH/H$_2$O$_2$ and MeOH/H$_2$O$_2$ fuel
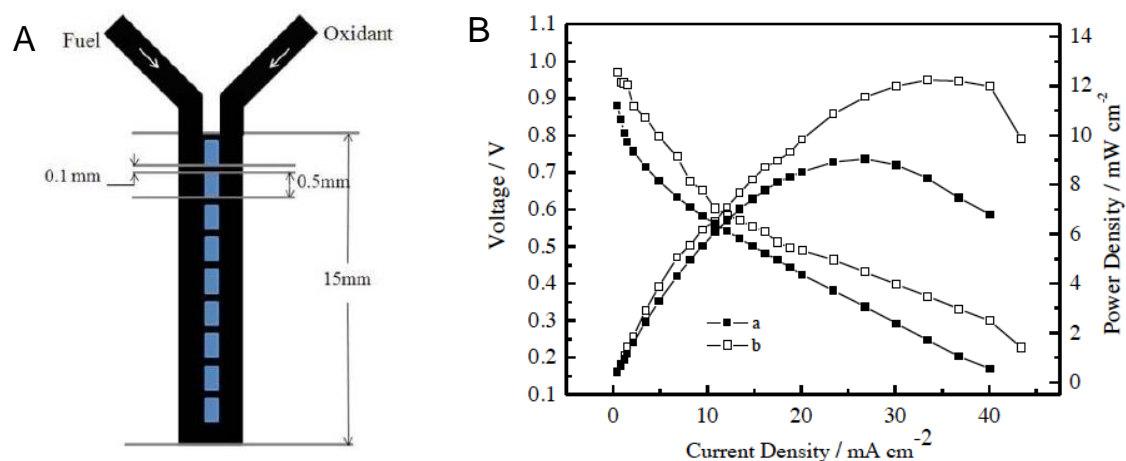

Fig. 3. (A) Schematic drawing of the ladder microchannel structure and (B) Polarization curves of the microfluidic MeOH/H$_2$O$_2$ fuel cell with (a) normal shaped microchannel and (b) ladder-shaped microchannel at 25 °C . The flow rates of anolyte and catholyte were 0.5 mL min^{-1}. [11]

cells were similar level of that of H_2O_2/H_2O_2 fuel cell, although the oxidation potentials of formic acid ($CO_2 + 2H^+ + 2e^- = HCOOH$; $E^o = -0.199$ V vs NHE) and methanol ($CO_2 + 2H_2 + 4 e^- = CH_3OH + H_2O$; $E^o = 0.03$ V vs NHE) were negative compared with that of H_2O_2 ($E^o = 0.682$ V).[10,11] These results indicate larger overpotentials are necessary for fuels oxidation at the anodes.

Several $NaBH_4$-H_2O_2 fuel cells employed Pt supported on carbon as the cathode together with Zn, $AuCo/TiO_2$-NTs, Ag needles or Pd supported on carbon as an anode.[13-17] High open circuit voltage of 3.0 V is predicted from negative oxidation potential of BH_4^- ($BH_4^- + 8OH^- = BO_2^- + 6H_2O + 8e^-$; $E^o = -1.24$ V vs NHE) and highly positive reduction potential of H_2O_2 ($E^o = 1.76$ V) under acidic conditions, which is higher than 1.23 V of H_2/O_2 fuel cells and 1.19 V of $MeOH/O_2$ fuel cells.[18] A $NaBH_4/H_2O_2$ fuel cell constructed with Pt supported on carbon as the cathode exhibited extremely high power density of 600 mW cm^{-2} with open circuit voltage of 1.3 V by supplying an aqueous solution containing 20% H_2O_2 and 5% phosphate as catholyte and that containing 20% $NaBH_4$ and 1.8 M NaOH as anolyte (Fig. 4).[18]
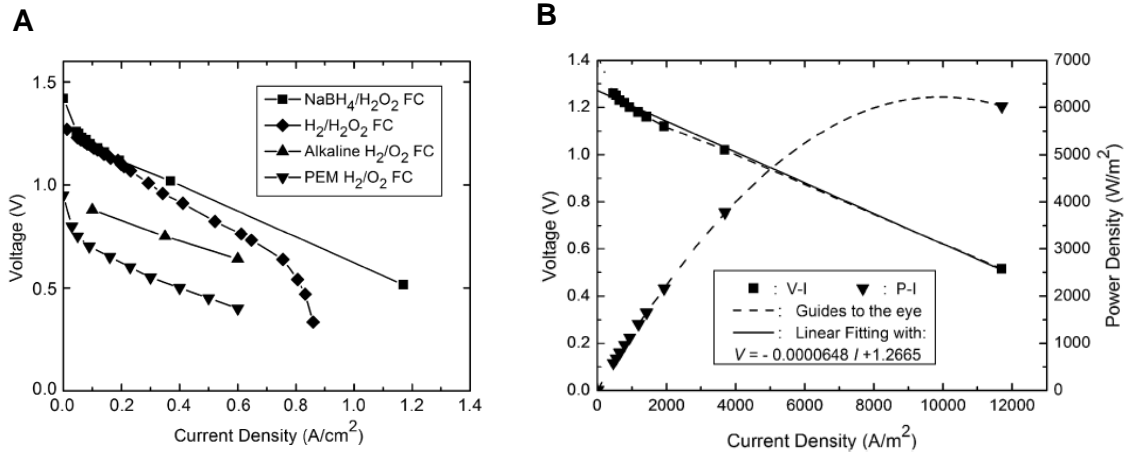

Fig. 4. (A) The *I-V* characteristics of $NaBH_4/H_2O_2$, H_2/H_2O_2, alkaline H_2/O_2 and H_2/O_2 PEM fuel cells operating at room temperature, and ambient pressure. The curve for the H_2/H_2O_2 fuel cell is tested with an acidic catholyte (pH 2). (B) Power density of the $NaBH_4/H_2O_2$ fuel cell.[18]

b. Au-Based Catalysts

Au based catalysts are used as cathodes of $NaBH_4/H_2O_2$, N_2H_4/H_2O_2 and Al/H_2O_2 fuel cells. $NaBH_4/H_2O_2$ fuel cells using Au as cathodes exhibit high power density ranging from 100 to 400 mW cm^{-2} as well as those using Pt as cathodes. Not only high catalytic activity for H_2O_2 reduction but also low activity for H_2O_2 decomposition made Au as a suitable cathode for the $NaBH_4/H_2O_2$ fuel cells, which was evidenced by catalysis examination of multiwall carbon nanotubes supporting Rh, Ru, Pt, Au, Ag, Pd, Ni, and Cu for both H_2O_2 reduction and H_2O_2 decomposition.[19]

The anodic reaction of Al/H_2O_2 fuel cells is as follows: $Al + 3OH^- = Al(OH)_3 + 3e^-$; $E^o = -2.30$ V, thus, the combination with the cathodic reaction ($HO_2^- + H_2O + 2e^- = 3OH^-$; $E^o = 0.87$ V) provides the overall voltage of 3.17 V.[19] A simple flow-path Al/H_2O_2 fuel cell using Al and Au plates as the anode and cathode, respectively, showed the maximum voltage around 1.4 V under the currents of 10^{-7} to 10^{-2} A in KOH solution (Fig. 5).[20]
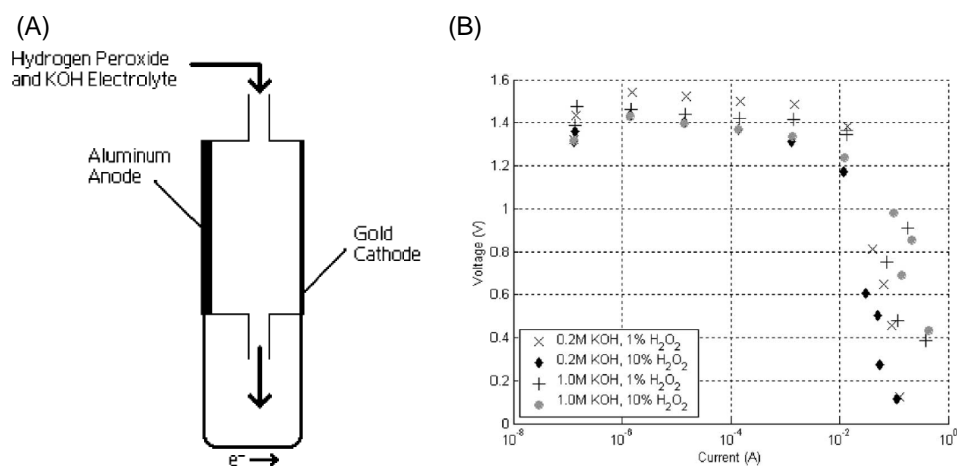

Fig. 5. (A) Single flow-path fuel-cell configuration and (B) voltage versus current graph for the concentration tests.[20]

N_2H_4 is an attractive fuel in N_2H_4/O_2 fuel cells, because the expected open circuit potential of N_2H_4 ($N_2H_4 + O_2 = N_2 + 2H_2O$; $E^o = 1.56$ V vs NHE) is higher than that of H_2/O_2 fuel cells (1.23 V).[21] N_2H_4/H_2O_2 fuel cells are expected to produce higher open

circuit voltage of 2.1 V under acidic conditions. A two-compartment N_2H_4/H_2O_2 fuel cell was constructed with nanoporous gold for both anode and cathode using an aqueous solution containing N_2H_4 and NaOH and an aqueous solution containing H_2O_2 and H_2SO_4 as the anolyte and catholyte, respectively.[22] The performance of the N_2H_4/H_2O_2 fuel cell highly depends on the concentrations of electrolytes in the anolyte and catholyte (Table 1).[22] The highest open circuit voltage of 1.02 V and maximum power density of 99 mW cm^{-2} were achieved by using an aqueous solution containing 4 M NaOH and 10 wt%N_2H_4 as an anolyte and that containing 0.5 M H_2SO_4 and 20%H_2O_2 as a catholyte at 60 °C.[22] The power density and open circuit voltage increased to 195.4 mW cm^{-2} and 1.21 V, respectively, by increasing the operation temperature to 80 °C.[22] Cell performance of the N_2H_4/H_2O_2 fuel cell employing nanoporous gold for both anode and cathode was superior to that employing Pt/C in terms of power density and open circuit voltage.[22] A N_2H_4/H_2O_2 fuel cell employing a Pt based anode and a Au/C cathode resulted in further improvement in both open circuit voltage (1.75 V) and power density (1.02 W cm^{-2}) as shown in Fig. 6.[23] The superior performance of the $NaBH_4/H_2O_2$ fuel cell using the Au cathode compared with that using the Pt cathode resulted from suppression of H_2O_2 decomposition on the Au electrode.

Table 1. Performance of N_2H_4/H_2O_2 fuel cells with various concentrations of electrolyte[22]

| Anolyte	Catholyte	OCV/V	MPD/mW cm^{-2}
4 M NaOH	0.05 M H_2SO_4	0.249	—
4 M NaOH	0.5 M H_2SO_4	0.489	—
4 M NaOH	1 M H_2SO_4	0.665	—
0.4 M NaOH	0.5 M H_2SO_4	0.334	—
0.04 M NaOH	0.5 M H_2SO_4	0.188	—
0.04 M NaOH+10% N_2H_4	0.5 M H_2SO_4+20% H_2O_2	0.531	16.44
0.4 M NaOH+10% N_2H_4	0.5 M H_2SO_4+20% H_2O_2	0.750	23.08
4 M NaOH+10% N_2H_4	0.5 M H_2SO_4+20% H_2O_2	1.025	99.47
4 M NaOH+10% N_2H_4	0.05 M H_2SO_4+20% H_2O_2	0.630	63.63

OCV: open circuit voltage, MPD: maximum power density
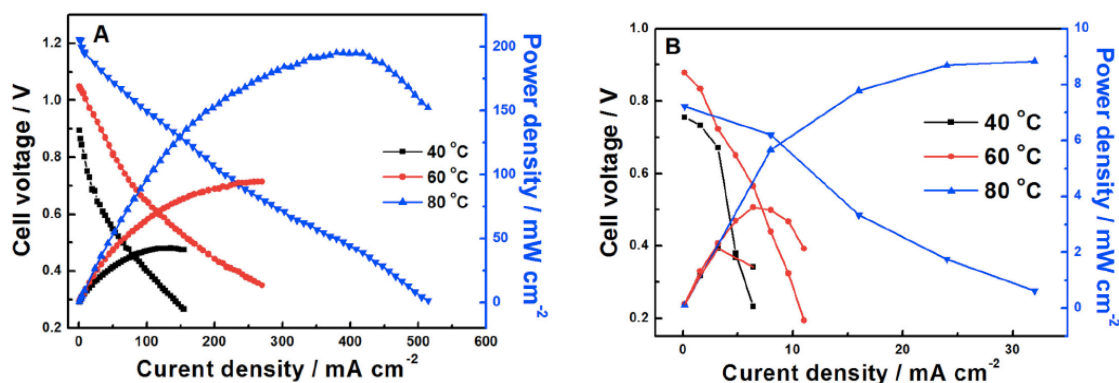
Fig. 6. Performance of a N_2H_4/H_2O_2 fuel cell at various temperatures with (A) nanoporous gold and (B) Pt/C as the catalysts for both anode and cathode, an aqueous solution of 4 M NaOH + 10 wt% N_2H_4 as the anolyte and that of 0.5 M H_2SO_4 +20 wt% H_2O_2 as the catholyte. The flow rates of the anolyte and catholyte were 1.4 and 4.2 mL min^{-1}, respectively.[22]

c. Pd-Based Catalysts

Pd cathodes were utilized in $NaBH_4/H_2O_2$, H_2O_2/H_2O_2, Al/H_2O_2 or Mg/H_2O_2, $HCOOH/H_2O_2$ and urea/H_2O_2 fuel cells.[10,24-29]

A H_2O_2/H_2O_2 fuel cell utilizing dendric Pd supported on carbon fiber cloth for both anode and cathode exhibited power density of 14.3 and 58.4 mW at 20 and 60 °C, respectively (Fig. 7).[25,26] The power density of the H_2O_2/H_2O_2 fuel cell was improved by replacing the dendric Pd supported on carbon anode with various types of Ni electrodes.[27-29] Especially, employment of Ni nanowire arrays as the anode resulted in the highest power density of 48.7 mW cm^{-2} at 20 °C.[29] Also, utilization of Ni supported on carbon fiber cloth (CFC) as the anode of a H_2O_2/H_2O_2 fuel cell resulted in 53.8 mW cm^{-2} at 50 °C.[28]

Pd-Ir alloy is used as cathodes of Al/H_2O_2 and Mg/H_2O_2 fuel cells.[30,31] An Al/H_2O_2 fuel cell using Pd-Ir as the cathode operated in an aqueous solution containing 3.0 M NaOH, 0.5 M H_2O_2 and 40 g L^{-1} sea salt at 55 °C. The Al/H_2O_2 fuel cell exhibited the open circuit voltage of 1.8 V and the maximum current density of 400 mA cm^{-2}.[31] The same Pd-Ir cathode was also used in Mg-H_2O_2 fuel cells. The oxidation
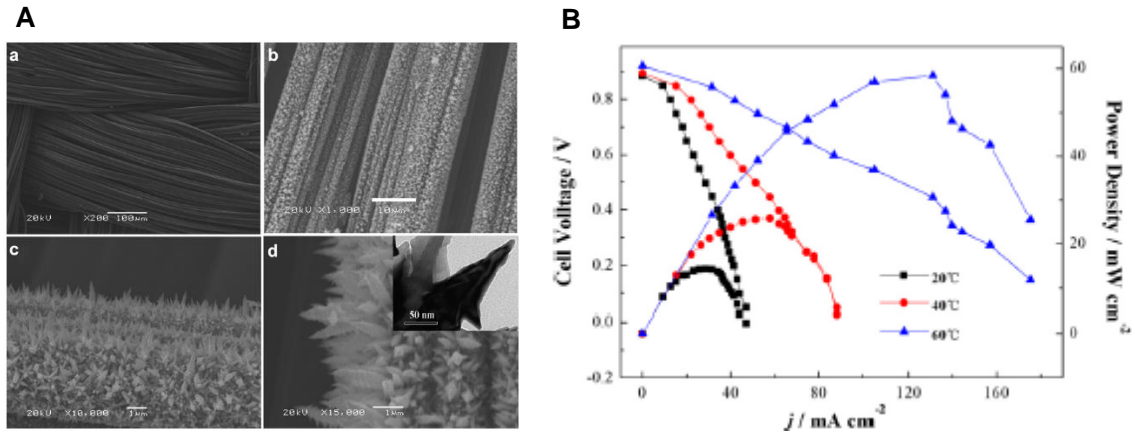
Fig. 7. (A) SEM images of CFC (a) and Pd/CFC (b, c and d) and TEM image of Pd (inset of d) and (B) Effect of operating temperature on the cell performance. Anolyte: 4.0 M KOH + 1.0 M H_2O_2. Catholyte: 2.0 M H_2SO_4 + 2.0 M H_2O_2. Flow rate: 10 mL min^{-1}).[25,26]

potential of Mg (Mg = Mg^{2+} + 2e$^-$; E^o = −2.37 V vs NHE) lower than that of Al (Al^{3+} + 3e$^-$ = Al; E^o = −1.68 V vs NHE) theoretically allows to construct high voltage fuel cells with open circuit voltage of 4.15 V.[32-34] A two-compartment Mg/H_2O_2 fuel cell employing a Mg wafer and Ir-Pd deposited on a carbon microfiber array as the anode and cathode, respectively, operated in an aqueous solution containing NaCl (40 g L^{-1}) for the anode and that containing H_2O_2, 0.2 M H_2SO_4 and NaCl (40 g L^{-1}) for the cathode (Fig. 8).[34] The output potential of the Mg/H_2O_2 fuel cell at low current density was ~2.0 V, and the maximum power density reached 84 mW cm^{-2}.[34] The power density can be increased to 200 mW cm^{-2} by increasing the operation temperature and concentration of H_2O_2 in the catholyte, however, significant H_2O_2 decomposition was observed on the cathode.[35]
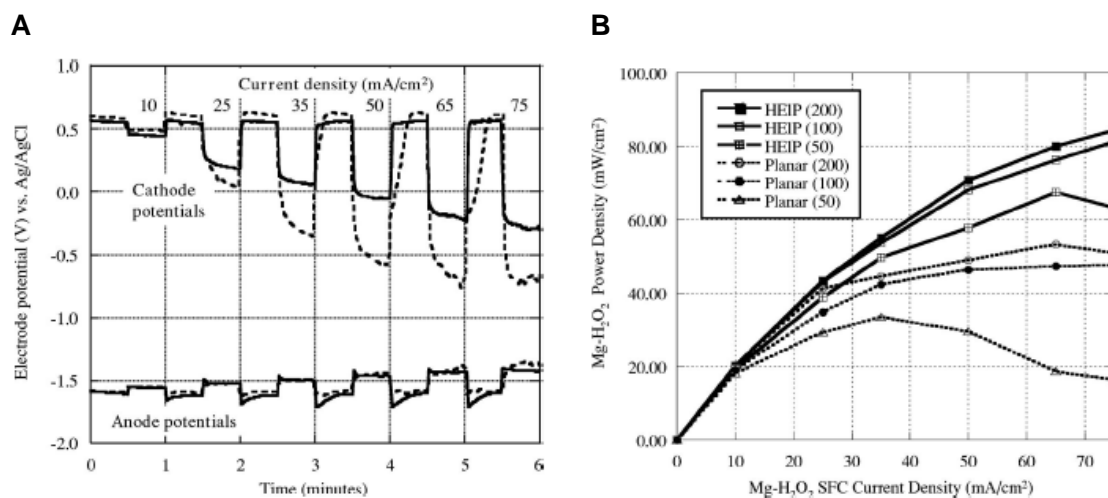
Fig. 8. (A) Mg–H_2O_2 fuel cell cathode and anode potentials at various current densities: [— : SFC with Ir-Pd deposited on a carbon microfiber array (HElP) cathode] and (- - -: SFC with a planar cathode).[34] (B) Power density of Mg–H_2O_2 fuel cell with HElP or planar cathodes. Catholyte flow rates in mL min^{-1} are given in parentheses. Anode flow rates were 200 mL min^{-1}.[34]

d. Ag-Based Catalysts

One-compartment fuel cells utilizing H_2O_2 as both fuel and oxidant were constructed with Ag and Au plates as cathode and anode, respectively.[36] Such a cell configuration is possible by employing selective electrodes for H_2O_2 reduction and oxidation. Measurements of cyclic voltammograms of H_2O_2 on Au, Ag, Pt, and Pd electrodes indicated both oxidation and reduction currents increased by the addition of H_2O_2.[36] The onset potential for H_2O_2 reduction on a Ag electrode (ca.−0.05V, Fig. 9A) was the highest among the electrodes although far below the thermodynamic value (0.73 V).[36] The onset potential for H_2O_2 oxidation on a Au electrode was lower than the onset potential for H_2O_2 reduction on a Ag electrode (Fig. 9B). This indicates that H_2O_2 oxidation by the Au electrode with H_2O_2 reduction by the Ag electrode can produce electric power. A one-compartment H_2O_2 fuel cell using Ag and Au plates as cathode and anode operated in an aqueous solution containing 1 M NaOH and 300 mM H_2O_2 successfully generated electrical power with the maximum current density of 2.9 mA cm^{-2} (Fig. 10).[36]
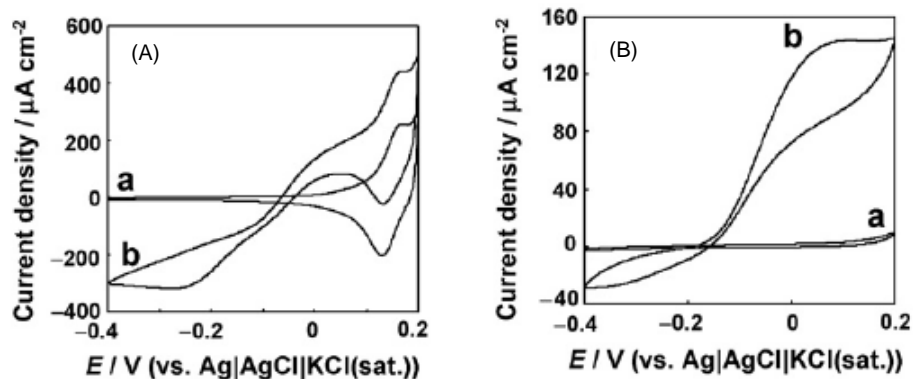
11

Fig. 9. Cyclic voltammograms of H_2O_2 on (A) Ag and (B) Au electrodes. Lines (a) and (b) indicate voltammograms in the absence and presence of H_2O_2, respectively. The measurements were performed in a 1 M NaOH solution under a nitrogen atmosphere. The concentration of H_2O_2 was fixed at 3 mM.[36]
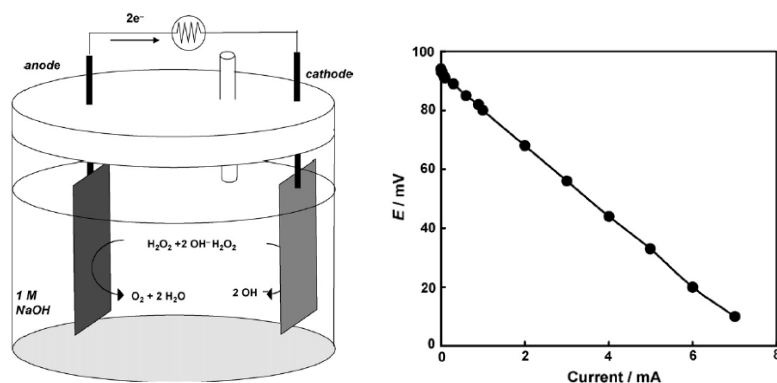

Fig. 10. *I‑V* curve of a one-compartment H_2O_2 fuel cell with Au anode‑Ag cathode. Performance tests were conducted in 1M NaOH solution containing 300 mM H_2O_2. The electrode surface areas are fixed at 2.4 cm^2.[36]

The one-compartment fuel cells utilizing H_2O_2 were also constructed with Ag-Pb alloy nanoparticles supported on a glassy carbon electrode as the cathode and Au plates as the anode.[37] Alloy formation of Ag with Pb, which was confirmed by TEM observations and X-ray diffraction patterns, reduced the overpotential of H_2O_2 reduction, resulting in increasing power density by 5 times (Fig. 11).[37]

Al/H_2O_2 fuel cells were constructed with a cathode composed of Ag electrodeposited on Ni foam.[38] The performance of an Al/H_2O_2 fuel cell using the Ag/Ni cathode was examined with an solution containing 0.5 M H_2O_2, 2.0 M NaOH and
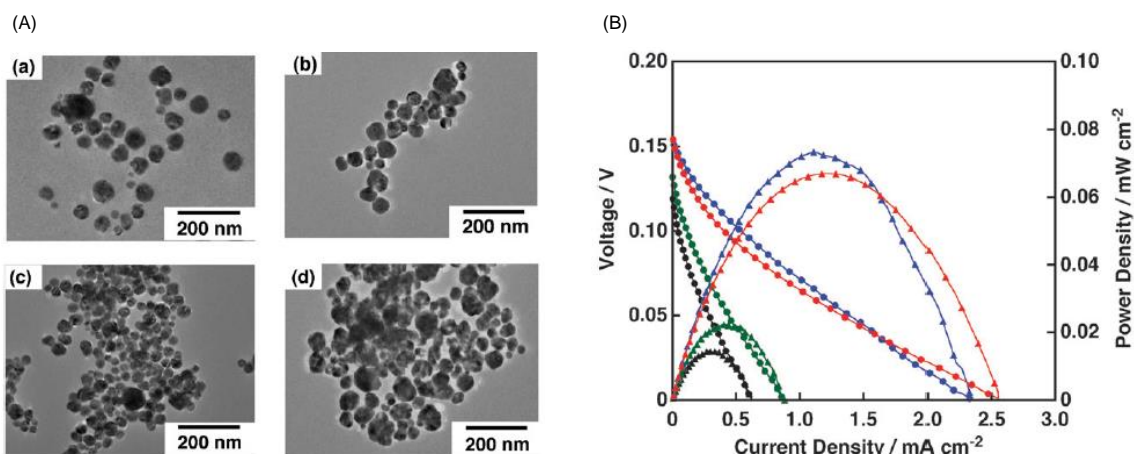
Fig. 11. (A) TEM images of Ag or Ag–Pb alloy nanoparticles. (a) Ag nanoparticles, (b) Ag–Pb alloy (Ag : Pb = 9 : 1), (c) Ag–Pb alloy (7 : 3) and (d) Ag–Pb alloy (Ag : Pb = 6 : 4). (B) $I–V$ and $I–P$ curves of a one-compartment H_2O_2 fuel cell with Ag or Ag–Pb alloy cathode. (Au anode. 1 M NaOH, 300 mM H_2O_2. Black: Ag, green: Ag : Pb = 6 : 4, red: Ag : Pb = 7 : 3 and blue: Ag : Pb = 9 : 1).[37]

40 g L^{-1} NaCl at 45 °C. The maximum power density of the Al/H_2O_2 fuel cell reached to 450 mWcm^{-2}.[38] When simple Ag mesh was employed as the cathode of the Al/H_2O_2 fuel cell instead of Ag/Ni cathode, the performance was significantly lowered. Cell voltage measured at 250 mAcm^{-2} for the Al/H_2O_2 fuel cell containing Ag catalyzed cathode was as much as 500 mV higher than that of planar Ag mesh (Fig. 12).[38] Thus, Ag-Ni interaction is beneficial to improve the catalysis for H_2O_2 reduction.[38]
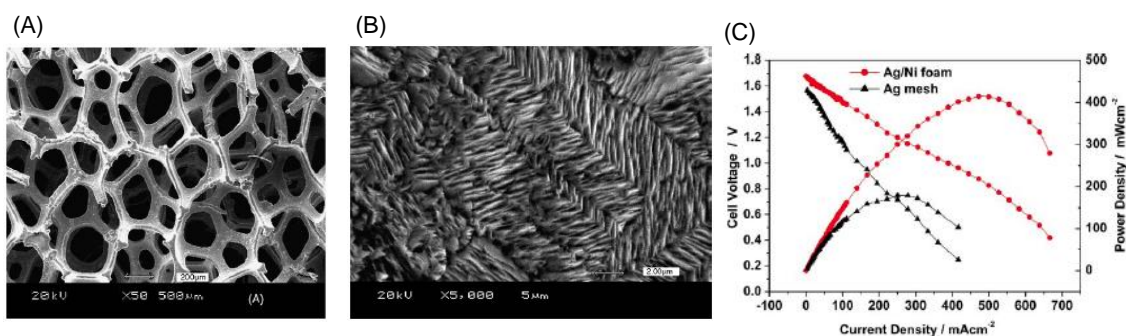

Fig. 12. SEM images of (A) Ni foam and (B) Ag/Ni foam. (C) Performance comparison of Al/H_2O_2 fuel cells with Ag/Ni and Ag mesh cathodes at 45 °C. Anode: 99.996% aluminum; electrolyte: 0.5M H_2O_2, 2.0M NaOH and 40 g L^{-1} NaCl.[38]

13

Catalysis of Ag/Ni electrode was further enhanced by combined with Pd metal in Mg-H_2O_2 fuel cells.[39] Pd was electrodeposited on Ag/Ni foam (Fig. 13). The content of deposited Pd was nearly double of Ag metal on the Ni form determined by EDS analysis.[39] Cathodic polarization behavior of Ag/Ni and Pd-Ag/Ni was compared at 20 and 50 °C. In both cases, electrode performance for H_2O_2 reduction was improved at higher temperature and Pd-Ag/Ni showed superior activity to Ag/Ni. As expected, the performance of Mg/H_2O_2 fuel cell constructed with Pd-Ag/Ni was better than that with Ag/Ni at the same operation temperature.[39] At 50 °C, the maximum power density of the fuel cell using Pd-Ag/Ni reached 140 mW cm^{-2}, on the other hand, that of Ag/Ni remained at 110 mW cm^{-2} (Fig. 14).[39]
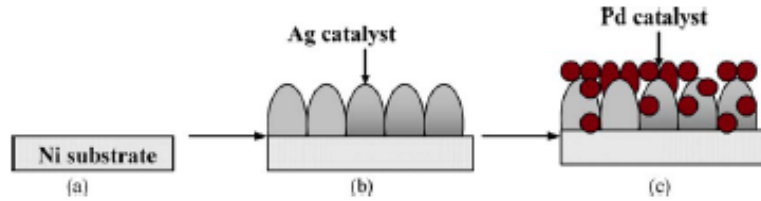

Fig. 13. Schematic of the preparation method of Pd-Ag catalyzed Ni foam electrode. (a) Ni foam, (b) Ag/Ni cathode and (c) Pd-Ag/Ni cathode.[39]
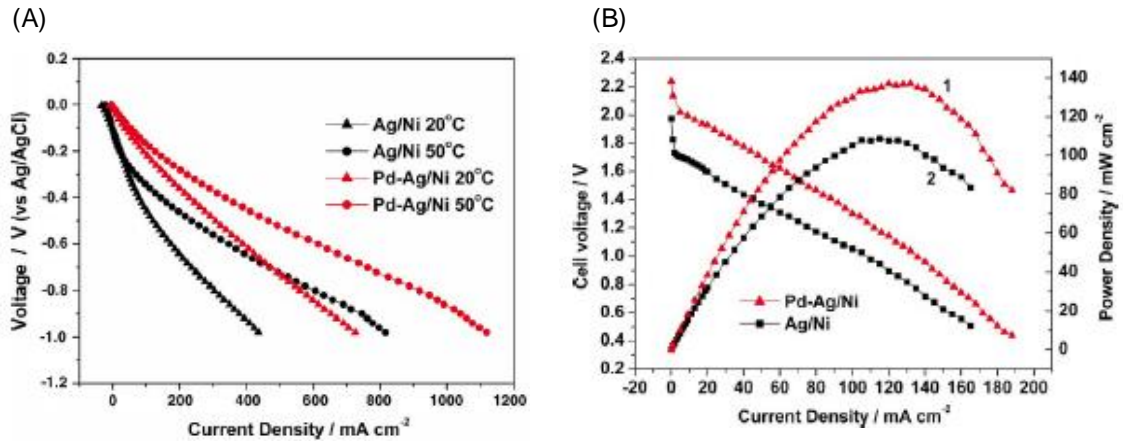

Fig. 14. (A) Polarization curves for Ag/Ni and Pd-Ag/Ni cathodes at 20 and 50 °C. Electrolyte: 0.5 M H_2O_2, 0.1 M H_2SO_4 and 40 g L^{-1} NaCl. (B) Performance comparison of Mg/H_2O_2 fuel cell with different cathodes at 50 °C. Anode: 99.96% Mg. Cathode: (1) Pd-Ag/Ni and (2) Ag/Ni. Anolyte: 40 g L^{-1} NaCl, 200 ml min^{-1}. Catholyte: 0.5M H_2O_2, 0.1 M H_2SO_4 and 40 g L^{-1}, NaCl, 100 ml min^{-1}.[39]

e. Ni-Based Catalysts

Rolled up Ni form was used as cathode of a Li/H_2O_2 semi-fuel cell with high stability longer than 800 h, which is suitable for electric vehicles applications (Fig. 15).[40] High output voltage of 4.83 V was expected for the cell because of very negative potential on Li ionization ($Li = Li^+ + e^-$, $E^o = -3.05$ V vs NHE) and very positive potential of H_2O_2 reduction ($H_2O_2 + 2H^+ + 2e^- = 2H_2O$, $E^o = 1.78$ V vs NHE).[40] However, the obtained discharge voltage was 2.7 V, which is comparable to that of $Li-O_2$ batteries.[40] A reason for the low voltage seemed to be undesired reaction on cathode as evidenced by lower open circuit potential of the cathode (~0.52 V), implying side reactions owing to O_2 contamination ($O_2 + 2H^+ + 2e^- = H_2O_2$, $E^o = 0.695$ V vs NHE or $O_2 + 2H_2O + 4e^- = 4OH^-$, $E^o = 0.401$ V).[40] More appropriate cathode suitable for H_2O_2 reduction without H_2O_2 decomposition should be chosen for this battery system.
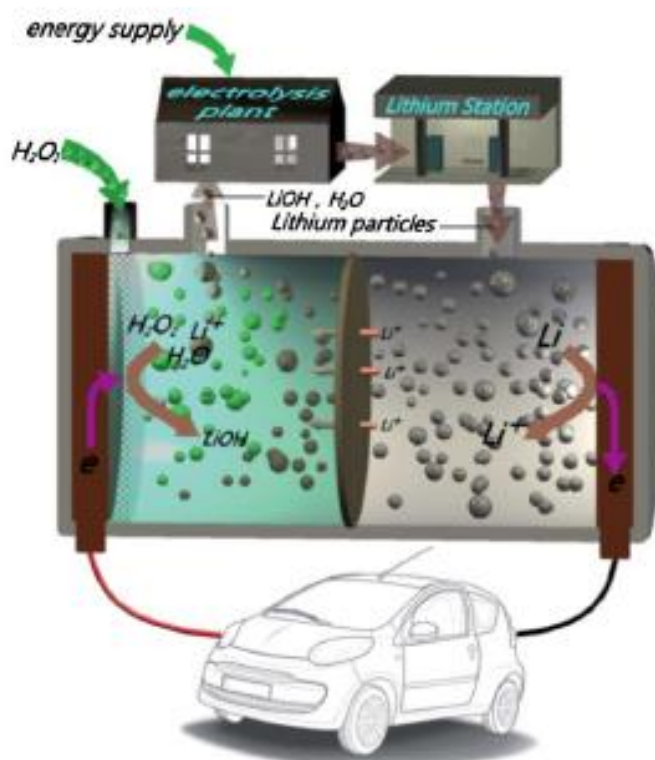

Fig. 15. A concept image for Li/H_2O_2 semi-fuel cell with a lithium recycle system for electric vehicles propulsion. Cars get refuelled in lithium stations; the only emission is LiOH, which can be used to fabricate metallic Li for fuel in plants.[40]

Metal-Oxide Catalysts

a. Co-Based Oxides

Assembly of Co_3O_4 nanowires supported on Ni-form has been utilized as the cathode of an Al/H_2O_2 fuel cell (Fig. 16).[41] The Al anode was supplied 3.0 M KOH solution and the catholyte contained 3.0 M KOH and $0.2 - 1.0$ M H_2O_2.[41] Cell performance with 0.4 M H_2O_2 catholyte improved by increasing the operation temperature, where the peak power density was 85 mW cm^{-2} at room temperature increased to 137 mW cm^{-2} at 65 °C (Fig. 17).[41] $La_{0.6}Ca_{0.4}CoO_3$ prepared by calcination at 650 °C has been employed instead of Co_3O_4/Ni as the cathode in the Al/H_2O_2 fuel cell. The power density of the cell exceeded 200 mW cm^{-2} at room temperature (Fig. 18).[42]

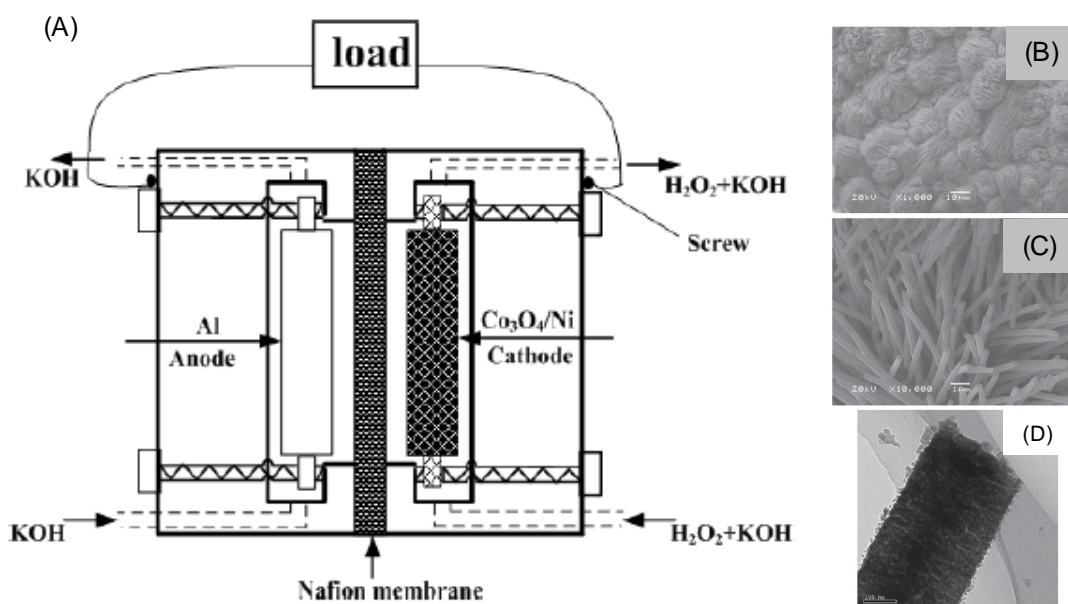**Fig. 16.** (A) A schematic representation of the Al/H_2O_2 fuel cell configuration (B, C) SEM images of the Co_3O_4/Ni cathode and (D) the TEM image of a single Co_3O_4 nanowire.[41]

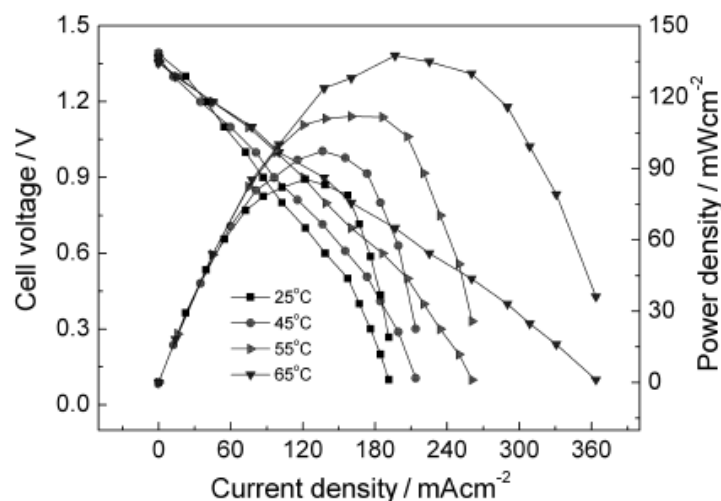**Fig. 17.** Effects of the operation temperature on the Al/H$_2$O$_2$ fuel cell performance. Anolyte: 3.0 M KOH. Catholyte: 3.0 M KOH + 0.4 M H$_2$O$_2$. Flow rate: 80 mL min^{-1}.[41]
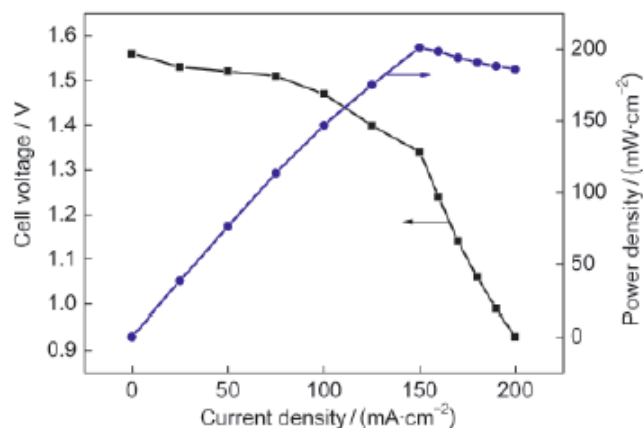

Fig.18. Performance of the Al/H$_2$O$_2$ fuel cell with La$_{0.6}$Ca$_{0.4}$CaO$_3$ cathode. Anolyte: 3.0 M KOH at a flow rate of 80 cm^3·min^{-1}; catholyte: 3.0 M KOH + 0.4 M H$_2$O$_2$; operation temperature: room temperature.[42]

b. Mn Oxide

Mn-based perovskite, La$_{0.7}$Sr$_{0.3}$MnO$_{3-\delta}$, was used as a cathode for constructing NaBH$_4$/H$_2$O$_2$ fuel cells with a Pt mesh as an anode.[43] Catalytic performance of La$_{0.7}$Sr$_{0.3}$MnO$_{3-\delta}$ for H$_2$O$_2$ reduction was compared with Co-based perovskite chosen

from LaCoO$_{3-\delta}$, La$_{0.84}$Sr$_{0.16}$CoO$_{3-\delta}$ and (La$_{0.8}$Sr$_{0.2}$)(Fe$_{0.8}$Co$_{0.2}$)O$_{3-\delta}$.[43] Electrochemical measurements of an electrode modified with a perovskite were performed in a solution containing 0.4 M H$_2$O$_2$ and 2 M NaOH (Fig. 19).[43] Among the electrodes tested,
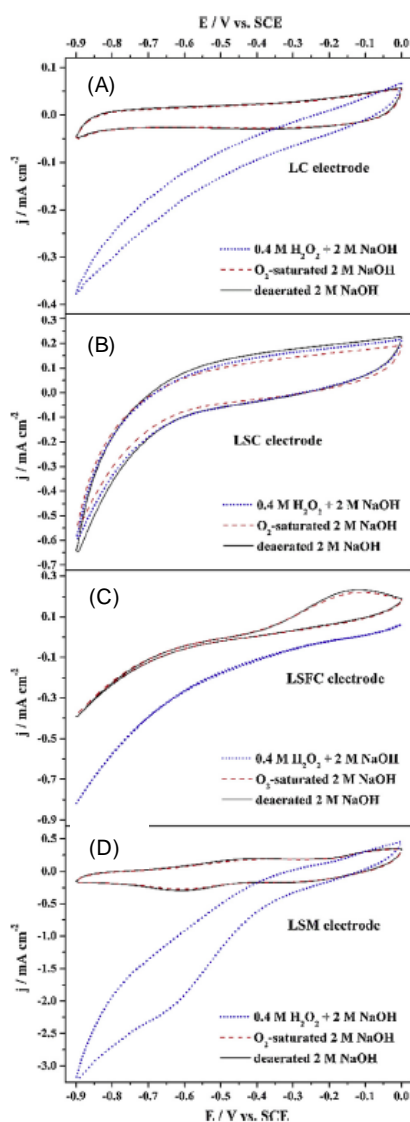

Fig. 19. Cyclic voltammograms of H$_2$O$_2$ on a perovskite cathode [(A) LaCoO$_{3-\delta}$, (B) La$_{0.84}$Sr$_{0.16}$CoO$_{3-\delta}$, (C) (La$_{0.8}$Sr$_{0.2}$)(Fe$_{0.8}$Co$_{0.2}$)O$_{3-\delta}$ and (D) La$_{0.7}$Sr$_{0.3}$MnO$_{3-\delta}$] in 2 M NaOH at 25 °C. Scan rate: 25 mVs^{-1}.[43]

La$_{0.7}$Sr$_{0.3}$MnO$_{3-\delta}$ exhibited the highest catalytic activity for H$_2$O$_2$ reduction.[43] Thus, an NaBH$_4$/H$_2$O$_2$ fuel cell was constructed with a Pt mesh and La$_{0.7}$Sr$_{0.3}$MnO$_{3-\delta}$ as an anode and cathode, respectively.[43] The cell performance measured at the temperatures ranging

from 25 to 45 °C indicated that power density increased in accordance with the increase of the operating temperature, although the cell performance at 25 °C was inferior to that of a fuel cell using Pt cathode instead of $La_{0.7}Sr_{0.3}MnO_{3-\delta}$ (Fig. 20).[43]
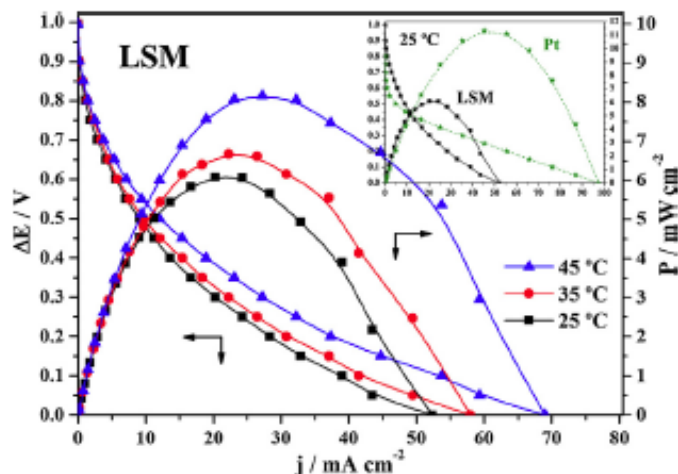

Fig. 20. Effect of temperature on the polarization behavior and corresponding peak power density curves for a DBPFC using LSM cathode. Inset shows direct comparison of the $La_{0.7}Sr_{0.3}MnO_{3-\delta}$ (LSM) and Pt cathodes at 25 °C.[43]

An $NaBH_4/H_2O_2$ fuel cell employing Pt/C and MnO_2 as an anode and a cathode, respectively, showed high power density and open circuit voltage. Optimization of an electrolyte (Nafion membrane), operating temperature, concentrations of $NaBH_4$ and NaOH, and H_2O_2 resulted in increasing the power density to 130 mW cm^{-2} under the conditions of Nafion 117, 80 °C, 1.0 M $NaBH_4$, 2 M NaOH, and 6.0 M H_2O_2 with the open circuit voltage of 1.3 V (Fig. 21).[44]

Metal Complexes

a. Cyano-Bridged Complexes

H_2O_2 reduction has been extensively studied for electrochemical sensors to detect H_2O_2 formation in biological cells. One of the most extensively studied material for this purpose is polymeric cyano-bridged metal complexes so called Prussian blue, $Fe^{III}[Fe^{II}(CN)_6]$, analogues (Fig. 22). [45-71]
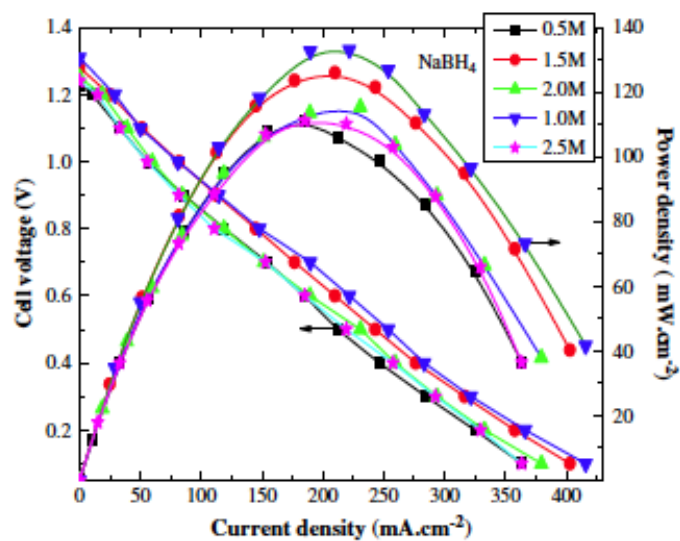
Fig. 21. Effect of NaBH$_4$ concentration on the cell voltage and power density–current density curves collected from NaBH$_4$/H$_2$O$_2$ fuel cell with a Nafion117 membrane at 80 °C: anode Pt/C (4.0 mg cm^{-2}), cathode MnO$_2$ (4.0 mg cm^{-2}), 2 M NaOH solution and 6.0 M H$_2$O$_2$ oxidant.[44]
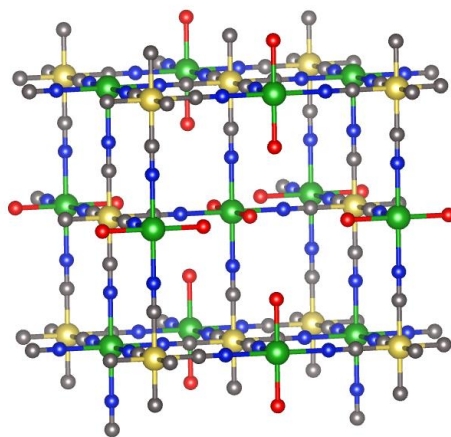

Fig. 22. A schematic drawing of a typical structure of Prussian blue

Prusssian-blue film electrodeposited on a Pt electrode was used as a cathode of direct borohydride fuel cells together with a Pt electrode as an anode. The fuel cells operated with an anolyte containing NaBH$_4$ and NaOH, and a catholyte containing H$_2$O$_2$

and HCl. The fuel cell operating 1.0 M $NaBH_4$ and 4.0 M NaOH as an anolyte and 5.0 M H_2O_2 and 1.5 M HCl as catholyte exhibited the highest power density of 206 mW cm^{-2} at a cell voltage of 0.80 V and a current density of 257 mA cm^{-2} at 65 °C (Fig. 23).[72]
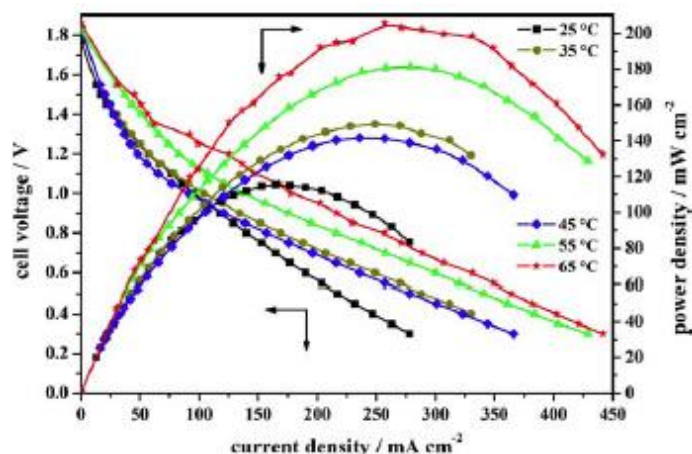

Fig. 23. Effect of the operation temperature on the current and power density of a $NaBH_4/H_2O_2$ fuel cell using a prussian blue supportted on Pt as a cathode. Fuel: 1.0 M $NaBH_4$ + 4.0M NaOH. Oxidant: 5.0 M H_2O_2 + 1.5M HCl.[72]

Prusssian blue nanoparticles supported on a carbon paper (10 mg cm^{-2}) by the spray drying method were used as a cathode of a one-compartment fuel cell using Ag or Ni as an anode. When the performance tests of the cells were examined with a solution containing 0.1 M HCl and 0.5 M H_2O_2, a maximum power densities were 0.8 and 1.55 mW with a silver anode and a Ni anode at 0.3 V, respectively (Fig. 24).[73]

The catalytic activity of Prussian blue for H_2O_2 reduction can be improved by replacing C-bound Fe ions with another metal ion such as Co(III) ion.[74] When $Fe_3[Co^{III}(CN)_6]_2$ was employed as a cathode to construct a one-compartment fuel cell with a Ni anode, the maximum power densities, which were 0.17 and 1.2 mW cm^{-2} under the conditions of pH 3 and 1, respectively, were double those of a fuel cell employing Prussian blue supported on a carbon paper (2 mg cm^{-2}) as a cathode (Fig. 25).[74] Inferior cell performance was observed when $Fe_3[Ir^{III}(CN)_6]_2$ or $Fe_3[Rh^{III}(CN)_6]_2$ was used as cathode instead of $Fe_3[Co^{III}(CN)_6]_2$ although no significant change in the crystal structures was observed.[74]
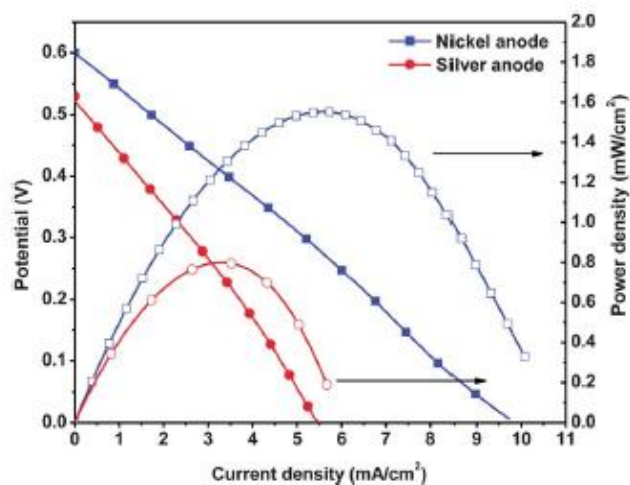
Fig. 24. Current–potential and current–power curves of the single compartment H_2O_2 fuel cell with nickel and silver anodes and unsupported PB coated on carbon paper as a cathode. Performance tests were carried out under acidic conditions using 0.1 M HCl and 0.5 M H_2O_2.[73]

Fig. 25. *I–V* (black) and *I–P* (gray) curves of a one-compartment H_2O_2 fuel cell with a Ni anode and a carbon-cloth electrode that was modified with a polycyanide complex: (A, C) $Fe^{III}_4[\{Fe^{II}(CN)_6\}_3]$ and (B, D) $Fe^{II}_3[\{Co^{III}(CN)_6\}_2]$. Performance tests were conducted in an aqueous solution of $HClO_4$ [(A, B): pH 3; (C, D): pH 1] that contained H_2O_2 (0.30 M) and NaCl (1.0 M). Currents and powers were normalized by a geometric surface area of electrode.[74]

The catalytic activity of polynuclear cyanide complexes for H_2O_2 reduction was effectively enhanced by modification of framework structure.[75] The window size of homoleptic polynuclear cyanide complexes, in which the C−N bond (1.13 Å) is shorter than the O−O bond of H_2O_2 (1.46 Å), can be expanded by the combination of a polynuclear cyanide complex forming a layered structure and a bridging extraligand larger than the cyanide ligand.[75] The 2D layers of $Fe[M(CN)_4]$ (M = Pt or Pd) connected with pyrazine molecules have been reported to have porous structure with a large opening window. The N···N distance of pyrazine is 2.80 Å, which is considerably longer than the C−N bond length of the cyanide ligand (1.13 Å). Also, pyrazine is known as a weakly bound ligand with a pK_b value of 13, so that the Fe^{2+} ions are expected to interact with H_2O_2 although the pyrazine molecules coordinate to Fe^{2+} ions.[75] The performance of a one-compartment fuel cells using H_2O_2 was evaluated with carbon-cloth cathodes mounting $Fe[M(CN)_4]$ (M = Pt or Pd) using the drop-casting method and a nickel mesh anode in an aqueous solution (HClO4, pH 1 or 3) that contained 0.30 M H_2O_2 at room temperature (Fig. 26a, b) .[75] The open-circuit potential

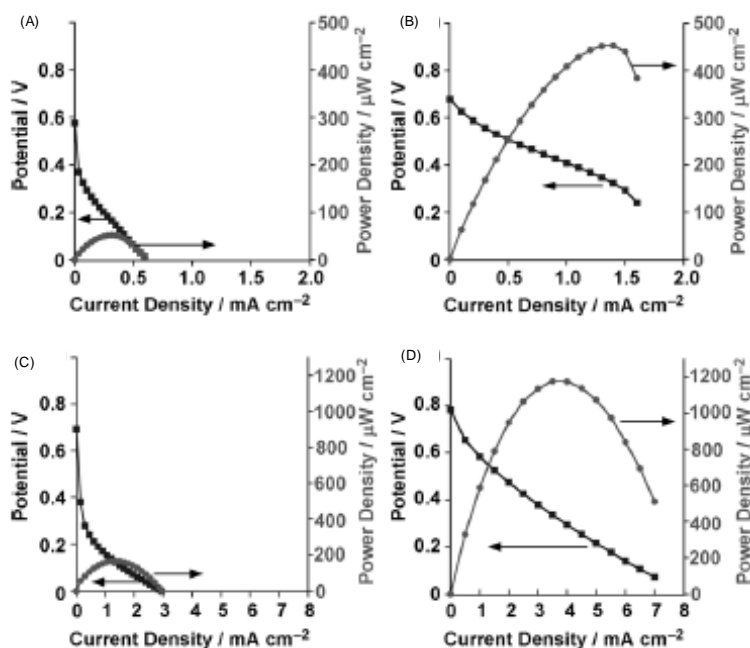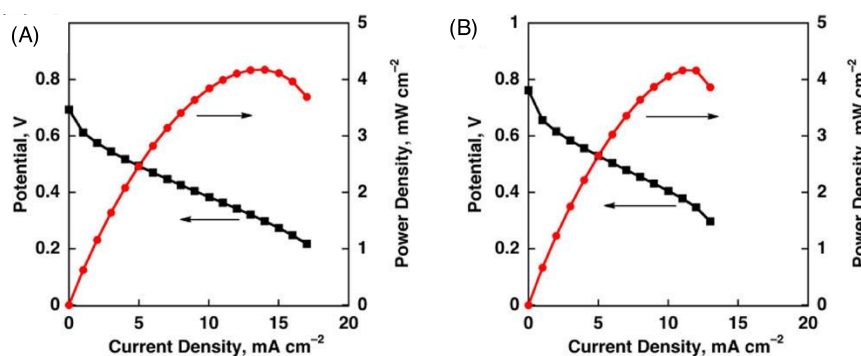**Fig. 26.** *I−V* (black) and *I−P* (red) curves of a one-compartment H_2O_2 fuel cell with a nickel anode and a carbon-cloth electrode modified with a pyrazine-bridged cyanide complexes pyrazine-bridged $Fe[M^C(CN)_4]$ complex [M^C = (A) Pt^{2+} and (B) Pd^{2+}]. Performance tests were conducted in an aqueous solution of HClO4 (pH 1) that contained H_2O_2 (0.30 M) and NaCl (1.0 M). Currents and powers were normalized by the geometric surface area of an electrode.[75]

of each H_2O_2 fuel cell operating at pH 1 was between 0.70 and 0.80 V. The power density of the H_2O_2 fuel cells with complexes containing Pt and Pd reached 4.2 mW cm^{-2}, which is more than double compared to the highest value (1.5 mW cm^{-2}) reported for one- compartment H_2O_2 fuel cells using homoleptic polymeric cyanide complexes. These results clearly indicate that using pyrazine as the bridging ligand improves the performance of the one-compartment H_2O_2 fuel cells in terms of power density.[75]

b. Porphyrin / Phthalocyanine Complexes

Iron tetramethoxy phenyl porphyrin (FeTMPP/C) was utilized as a cathode to build direct borohydride fuel cells employing the AB_5-alloy (Mm $Ni_{3.55}Al_{0.3}Mn_{0.4}Co_{0.75}$, Mm = Mischmetal) supported on carbon as an anode catalysts. The fuel cell operated with an aqueous solution containing 10 wt% $NaBH_4$ and 20 wt% NaOH as an anolyte and that containing 0.5 M H_2O_2 and 0.5 M H_2SO_4 as a catholyte at temperatures between 30 and 70 °C.[76] Cyclic voltammograms of H_2O_2 in an acidic solution were measured with FeTMPP/C electrode showed that the onset potential for H_2O_2 reduction is ~0.8 V. [76] Maximum power densities of the fuel cell operating at the temperatures at 30, 50 and 70 °C reached 18, 53 and 82 mW cm^{-2} at respective cell potentials of 0.5, 0.53 and 0.5 V, respectively (Fig. 27). [76]

Not only porphyrin but also phthalocyanine (Pc) was also used as cathode of a one-compartment H_2O_2 fuel cell using Ni as an anode.[77] The performance of the fuel cell was examined in buffer solutions containing 300 mM H_2O_2 at pH 3-5.[77] The maximum power density remained lower than 1 μW cm^{-2} at pH 4-5, however, the maximum power density exceeded 10 μW cm^{-2} at pH 3 (Fig. 28).[77] Such pH dependence was not observed for the fuel cells employing porphyrin compounds as cathode catalysts.[77] The improvement of the catalytic activity at lower pH resulted from the molecular structure of the phthalocyanine ligand, which possesses nitrogens at mesopositions.[77] Protonation to the nitrogens at lower pH, which was evidenced by an acid titration of $[Fe^{III}(Pc)Cl]$ (Fig. 29), effectively increased the reducing activity for
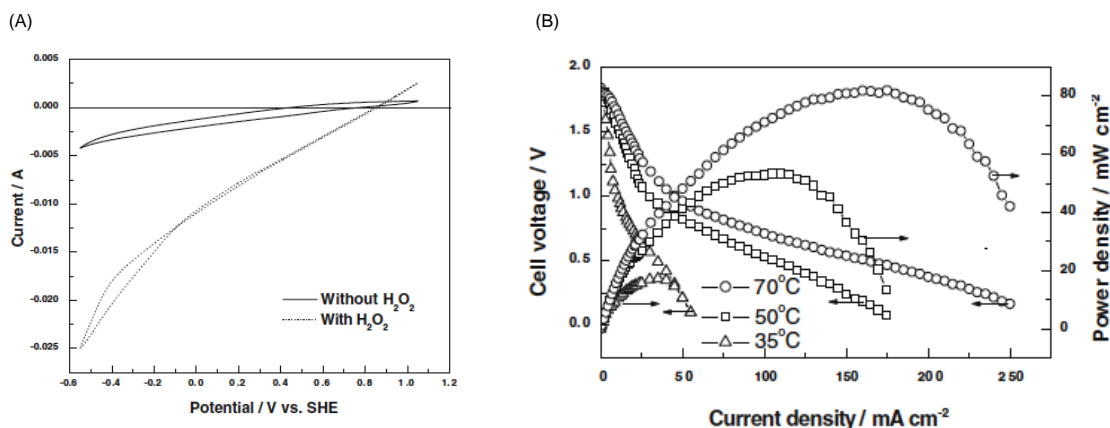
Fig. 27. (A) Cyclic voltammograms of H₂O₂ on the FeTMPP/C electrode in aqueous 0.5 M sulfuric acid with and without 0.5 M H₂O₂ and (B) Cell polarization curves for the NaBH₄/H₂O₂ fuel cell with FeTMPP/C cathode operating at temperatures between 30 and 70 °C with alkaline aq. NaBH₄ as an anolyte and an aqueous solution of 0.5 M H₂O₂ and 0.5 M sulfuric acid as a catholyte.[76]
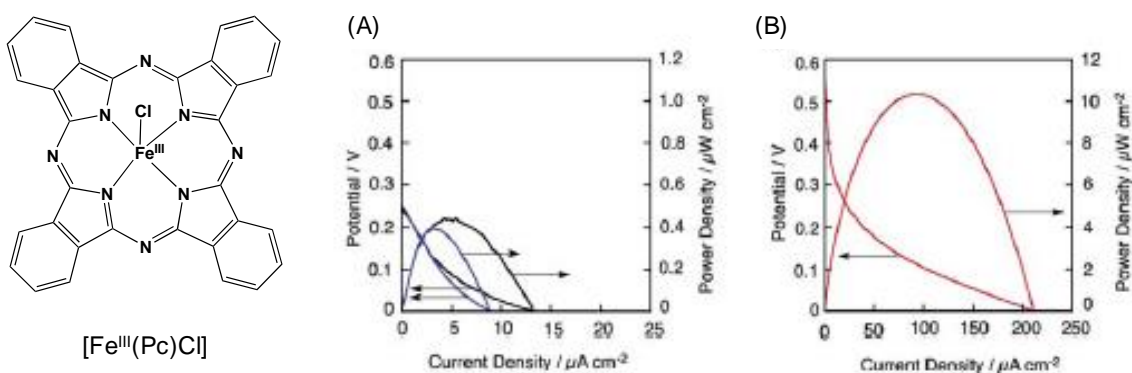
Fig. 28. *I–V* and *I–P* curves of a one-compartment H₂O₂ fuel cell with Ni anode and [Fe^{III}(Pc)Cl] cathode. Performance tests were conducted in an acetate buffer containing 300 mM H₂O₂. The pH of the solutions was fixed to 5 (a, blue), 4 (a, black) or 3 (b, red). Currents and powers were normalized by a geometric surface area of electrode.[77]
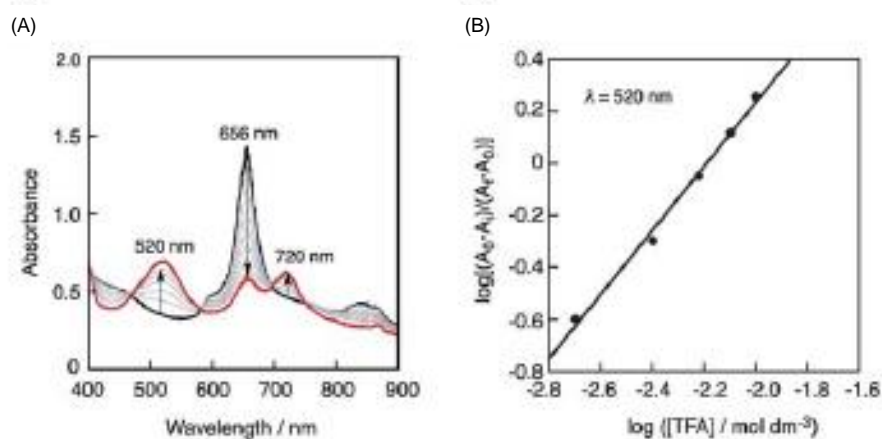
Fig. 29. (A) UV-vis absorption change of a benzonitrile solution of [Fe^{III}(Pc)Cl] (0.04 mM) by adding trifluoroacetic acid (2–16 mM). (B) The Hill plot obtained by absorption change at 520 nm.[77]

H$_2$O$_2$ because the protonation induces the positive shift of the redox potential of [Fe$^{II/III}$(Pc)Cl] to stabilize the Fe^{II} state.[77]

Others

a. Carbon A Mg-H$_2$O$_2$ fuel cell was constructed with noble metal free carbon based cathode. [78] A schematic drawing of the Mg/H$_2$O$_2$ fuel cell is indicated in Fig. 30. Two
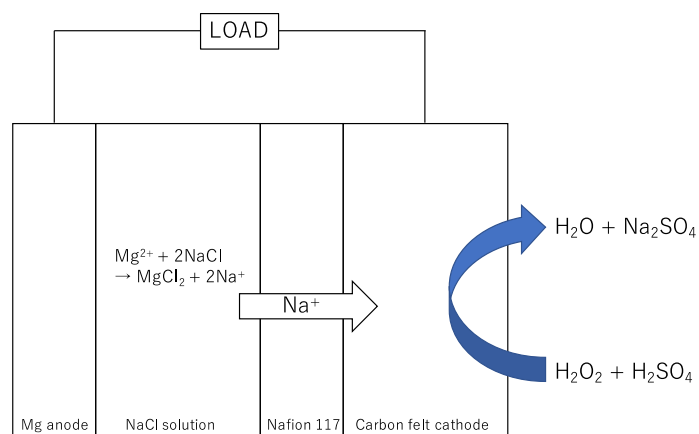

Fig. 30. Schematic drawing of a Mg/H$_2$O$_2$ fuel cell using carbon felt as the cathode.[78]

chambers were separated by Nafion 117, which acts as Na$^+$ ion conductor.[78] The chamber for Mg alloy (AZ61) anode contains 0.6 M NaCl solution and that for carbon

cloth or carbon felt cathode was supplied catholyte containing 2.0 M H_2O_2 and 2.0 M H_2SO_4 with flow rate of 50 mL min^{-1}.[78] Although both carbon cloth and carbon felt acted as cathodes, carbon felt exhibited smaller cathodic polarization. Power density of the cell reached 91 mW cm^{-2} and maintained for 26 h under optimized conditions.[78]

b. PbSO_4 $PbSO_4$ was employed as an active component of cathodes in a $NaBH_4/H_2O_2$ and H_2O_2/H_2O_2 fuel cells. Catalytic activity of $PbSO_4$ supported on carbon (Vulcan XC-72R) for H_2O_2 reduction was examined in 0.5 M sulfuric acid.[76] The reduction of H_2O_2 started at 0.75 V as indicated in Fig. 31A.[76] The $NaBH_4/H_2O_2$ fuel cell using
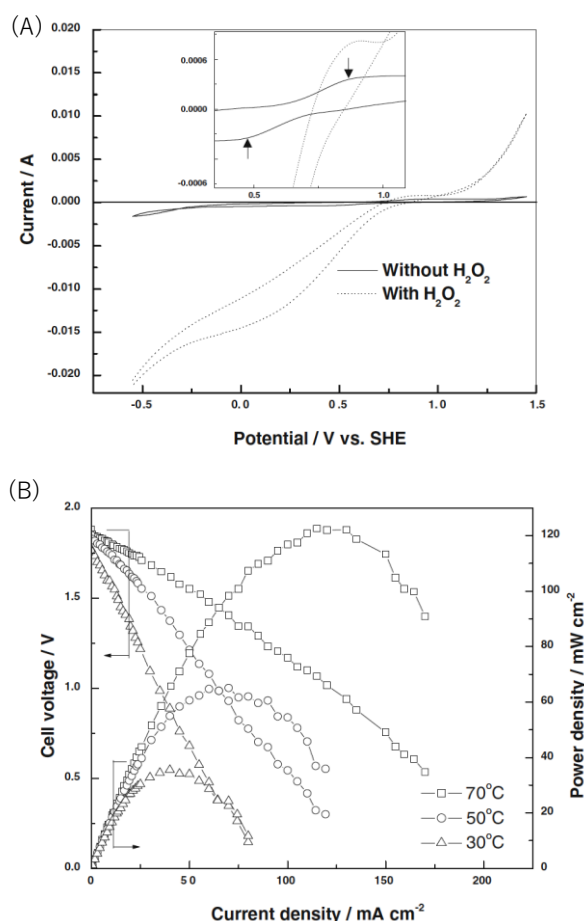

Fig. 31. (A) Cyclic voltammograms of H_2O_2 on a $PbSO_4$/C electrode in aqueous sulfuric acid with and without 0.5 M H_2O_2. (B) Cell polarization data for the fuel cell operating at temperatures between 30 and 70 °C with feeding alkaline aq. $NaBH_4$ and 0.5 M H_2O_2 in 0.5 M sulfuric acid solution to the anode and cathode, respectively.[76]

PbSO$_4$/C and AB$_5$ alloy composed of Ni, Al, Mn and Co showed the maximum power density of 120 mW cm^{-2} operating at 70 °C (Fig. 31B).[76]

PbSO$_4$ supported on carbon paper (PbSO$_4$/CP) prepared by electroless deposition was employed as the cathode of a H$_2$O$_2$/H$_2$O$_2$ fuel cell together with Ni anode.[3] The fuel cell used a basic H$_2$O$_2$ solution (3 M KOH + 1 M H$_2$O$_2$) as an anolyte and an acidic H$_2$O$_2$ solution (1.5 M H$_2$SO$_4$ + 1 M H$_2$O$_2$) as a catholyte. The power density obtained from the fuel cell (10 mW cm^{-2}) was more than double that of a fuel cell using Pt/CP cathode instead of PbSO$_4$/CP (4 mW cm^{-2}), suggesting that PbSO$_4$ is a better catalyst than Pt for electroreduction of H$_2$O$_2$ (Fig. 32).[3]
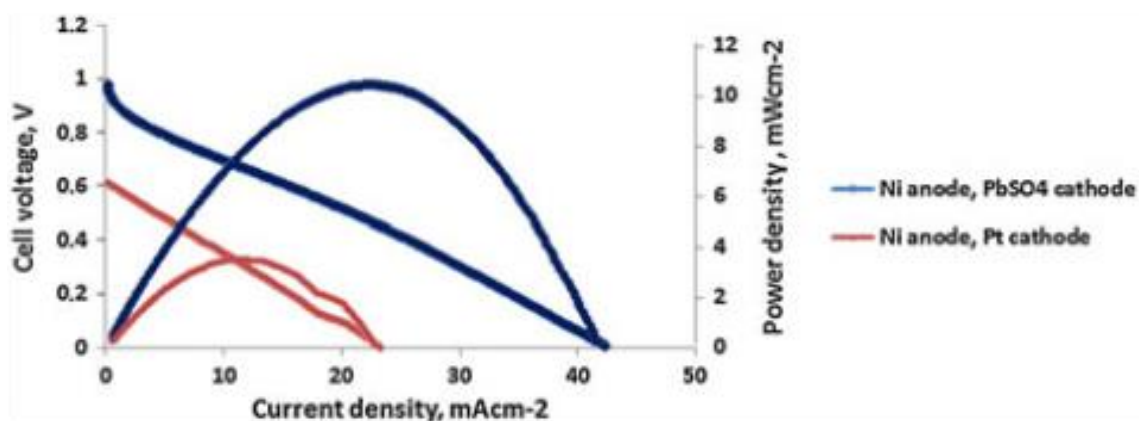
Fig. 32. Polarization curves and power curves of a passive H$_2$O$_2$/H$_2$O$_2$ fuel cell constructed with Ni/C anode and PbSO$_4$/C (solid circle) and Pt/C (frame circle) cathodes. Operating conditions: 3 M KOH + 1 M H$_2$O$_2$ as anolyte and 1.5 M H$_2$SO$_4$ + 1 M H$_2$O$_2$ as catholyte at 25 °C.[3]

Conclusion

Various types of fuel cells were constructed by employing metal, metal oxide and metal complexes as cathodes, where electrochemical H$_2$O$_2$ reduction proceeds. Molecular oxygen (O$_2$) often used as an oxidant for contracting fuel cells is abundant and free of charge, however, oxygen reduction involves four electrons and four protons to form two water molecules that is hard reaction from the kinetic point of view. H$_2$O$_2$ produced by two electron reduction of O$_2$ is more easily reduced to water by

two-electron reduction ($H_2O_2 + 2H^+ + 2e^- = 2H_2O$; $E^o = 1.78$ V vs NHE) than O_2 ($O_2 + 4H^+ + 4e^- = 2H_2O$; $E^o = 1.23$ V vs NHE) from both kinetic and thermodynamic points of views. The high reduction potential is beneficial to construct fuel cells with high power density and high voltage. In fact, some fuel cells using metal anode or borohydride fuel accomplished high power density and voltages. However, a couple of problems should be overcome to extend this success to other fuel cells. For examples, many cathodes show catalytic activity not only for H_2O_2 reduction but also for H_2O_2 decomposition by disproportionation. Additionally, H_2O_2 is a strong oxidizer that can corrode organic parts of fuel cells, probably because of formation of highly reactive $OH^\bullet$ by the one-electron reduction of H_2O_2. Negative potential of one-electron reduction of H_2O_2 ($H_2O_2 + H^+ + e^- = OH^\bullet + H_2O$; $E^o = 1.14$ V vs NHE) compared with two electron reduction indicates one-electron reduction is thermodynamically unfavorable, however, one-electron reduction may occur faster than two-electron reduction. Not only active but also selective cathodes for two-electron reduction of H_2O_2 should be developed to achieve high power fuel cells using H_2O_2 as an oxidant. Suitable catalysts for two-electron reduction of H_2O_2 would be found in electrodes used in H_2O_2 detection sensors but not used in fuel cells, such as shape-controlled metal nanoparticles,[79,80] graphene based materials,[81-83] polyoxometalate,[84-88] and metal complexes.[89,90]

Acknowledgements

References

(1) Bard, A. J.; Parsons, R.; Jordan, J. ed. *Standard Potentials in Aqueous Solution*; Marcel Dekker, 1985.

(2) Disselkamp, R. S. *Energy Fuels* **2008**, *22*, 2771.

(3)   Sanli, A. E. *Int. J. Energy Res.* **2013**, *37*, 1488.

(4)   Fukuzumi, S.; Yamada, Y.; Karlin, K. D. *Electrochim. Acta* **2012**, *82*, 493.

(5)   Fukuzumi, S.; Yamada, Y. *ChemElectroChem* **2016**, *3*, 1978.

(6)   Isaka, Y.; Oyama, K.; Yamada, Y.; Suenobu, T.; Fukuzumi, S. *Catal. Sci. Technol.* **2016**, *6*, 681.

(7)   Shiraishi, Y.; Kanazawa, S.; Kofuji, Y.; Sakamoto, H.; Ichikawa, S.; Tanaka, S.; Hirai, T. *Angew. Chem. Int. Ed.* **2014**, *53*, 13454-13459.

(8)   Mase, K.; Yoneda, M.; Yamada, Y.; Fukuzumi, S. *Nat. Commun.* **2016**, *7*.

(9)   Hasegawa, S.; Shimotani, K.; Kishi, K.; Watanabe, H. *Electrochem. Solid-State Lett.* **2005**, *8*, A119.

(10)   Kjeang, E.; Brolo, A. G.; Harrington, D. A.; Djilali, N.; Sinton, D. *J. Electrochem. Soc.* **2007**, *154*, B1220.

(11)   Huo, W. W.; Zhou, Y.; Zhang, H. F.; Zou, Z. Q.; Yang, H. *Int. J. Electrochem. Sci.* **2013**, *8*, 4827.

(12)   Sangarunlert, W.; Sukchai, S.; Pongtornkulpanich, A.; Nathakaranakule, A.; Luschtinetz, T. *J. Fuel Cell Sci. Technol.* **2011**, *8*.

(13)   Santos, D. M. F.; Sequeira, C. A. C. *J. Electrochem. Soc.* **2010**, *157*, B13.

(14)   Santos, D. M. F.; Balciunaite, A.; Tamasauskaite-Tamasiunaite, L.; Zabielaite, A.; Jagminiene, A.; Stankeviciene, I.; Naujokaitis, A.; Norkus, E. *J. Electrochem. Soc.* **2016**, *163*, F1553.

(15)   Wang, Y. G.; He, P.; Zhou, H. S. *Energy Environ. Sci.* **2010**, *3*, 1515.

(16)   Sanli, A. E.; Aksu, M. L.; Uysal, B. Z. *Int. J. Hydrogen Energy* **2011**, *36*, 8542.

(17)   Kim, J.; Jang, B.; Lee, T.; Kwon, S. *Int. J. Tubo Jet-Engines* **2015**, *32*, 291.

(18)   Luo, N.; Miley, G. H.; Gimlin, R.; Burton, R.; Rusek, J.; Holcomb, F. *J. Propul. Power* **2008**, *24*, 583.

(19)   Oh, T. H.; Jang, B.; Kwon, S. *Int. J. Hydrogen Energy* **2014**, *39*, 6977.

(20)   Brodrecht, D. J.; Rusek, J. J. *Appl. Energy* **2003**, *74*, 113.

(21)   Serov, A.; Kwak, C. *Appl. Catal., B* **2010**, *98*, 1.

(22)   Yan, X. L.; Meng, F. H.; Xie, Y.; Liu, J. G.; Ding, Y. *Sci. Rep.* **2012**, *2*.

(23)   Lao, S. J.; Qin, H. Y.; Ye, L. Q.; Liu, B. H.; Li, Z. P. *J. Power Sources* **2010**, *195*, 4135.

(24)   Guo, F.; Cheng, K.; Ye, K.; Wang, G. L.; Cao, D. X. *Electrochim. Acta* **2016**, *199*, 290.

(25) Yang, F.; Cheng, K.; Liu, X. L.; Chang, S.; Yin, J. L.; Du, C. Y.; Du, L.; Wang, G. L.; Cao, D. X. *J. Power Sources* **2012**, *217*, 569.

(26) Yang, F.; Cheng, K.; Mo, Y. H.; Yu, L. Q.; Yin, J. L.; Wang, G. L.; Cao, D. X. *J. Power Sources* **2012**, *217*, 562.

(27) Yang, F.; Cheng, K.; Xue, X.; Yin, J. L.; Wang, G. L.; Cao, D. X. *Electrochim. Acta* **2013**, *107*, 194.

(28) Yang, F.; Cheng, K.; Xiao, X.; Yin, J. L.; Wang, G. L.; Cao, D. X. *J. Power Sources* **2014**, *245*, 89.

(29) Ye, K.; Guo, F.; Gao, Y. Y.; Zhang, D. M.; Cheng, K.; Zhang, W. P.; Wang, G. L.; Cao, D. X. *J. Power Sources* **2015**, *300*, 147.

(30) Dow, E. G.; Bessette, R. R.; Seeback, G. L.; Marsh-Orndorff, C.; Meunier, H.; VanZee, J.; Medeiros, M. G. *J. Power Sources* **1997**, *65*, 207.

(31) Bessette, R. R.; Cichon, J. M.; Dischert, D. W.; Dow, E. G. *J. Power Sources* **1999**, *80*, 248.

(32) Bessette, R. R.; Medeiros, M. G.; Patrissi, C. J.; Deschenes, C. M.; LaFratta, C. N. *J. Power Sources* **2001**, *96*, 240.

(33) Medeiros, M. G.; Bessette, R. R.; Deschenes, C. M.; Patrissi, C. J.; Carreiro, L. G.; Tucker, S. P.; Atwater, D. W. *J. Power Sources* **2004**, *136*, 226.

(34) Patrissi, C. J.; Bessette, R. R.; Kim, Y. K.; Schumacher, C. R. *J. Electrochem. Soc.* **2008**, *155*, B558.

(35) Shu, C. Z.; Wang, E. D.; Jiang, L. H.; Tang, Q. W.; Sun, G. Q. *J. Power Sources* **2012**, *208*, 159.

(36) Yamazaki, S. I.; Siroma, Z.; Senoh, H.; Loroi, T.; Fujiwara, N.; Yasuda, K. *J. Power Sources* **2008**, *178*, 20.

(37) Yamada, Y.; Fukunishi, Y.; Yamazaki, S.; Fukuzumi, S. *Chem. Commun.* **2010**, *46*, 7334.

(38) Yang, W.; Yang, S.; Sun, W.; Sun, G.; Xin, Q. *J. Power Sources* **2006**, *160*, 1420.

(39) Yang, W. Q.; Yang, S. H.; Sun, W.; Sun, G. Q.; Xin, Q. *Electrochim. Acta* **2006**, *52*, 9.

(40) Liu, K.; Wang, C. A.; Ma, J. T. *RSC Adv.* **2014**, *4*, 18894.

(41) Lei, T.; Tian, Y. M.; Wang, G. L.; Yin, J. L.; Gao, Y. Y.; Wen, Q.; Cao, D. X. *Fuel Cells* **2011**, *11*, 431.

(42) Zhuang, S. X.; Liu, S. Q.; Zhang, J. B.; Tu, F. Y.; Huang, H. X.; Huang, K. L.; Li,

Y. H. *Acta Phys.-Chim. Sin.* **2012**, *28*, 355.

(43) Santos, D. M. F.; Gomes, T. F. B.; Sljukic, B.; Sousa, N.; Sequeira, C. A. C.; Figueiredo, F. M. L. *Electrochim. Acta* **2015**, *178*, 163.

(44) Wu, H. J.; Wang, C.; Liu, Z. X.; Mao, Z. Q. *Int. J. Hydrogen Energy* **2010**, *35*, 2648.

(45) Karyakin, A. A.; Karyakina, E. E.; Gorton, L. *J. Electroanal. Chem.* **1998**, *456*, 97.

(46) Karyakin, A. A.; Karyakina, E. E.; Gorton, L. *Electrochem. Commun.* **1999**, *1*, 78.

(47) Eftekhari, A. *Talanta* **2001**, *55*, 395.

(48) Karyakin, A. A. *Electroanalysis* **2001**, *13*, 813.

(49) Zhao, G.; Feng, J. J.; Zhang, Q. L.; Li, S. P.; Chen, H. Y. *Chem. Mater.* **2005**, *17*, 3154.

(50) Kumar, S. M. S.; Pillai, K. C. *Electrochem. Commun.* **2006**, *8*, 621.

(51) Qiu, J.-D.; Peng, H.-Z.; Liang, R.-P.; Li, J.; Xia, X.-H. *Langmuir* **2007**, *23*, 2133.

(52) Yu, H.; Sheng, Q. L.; Zheng, J. B. *Electrochim. Acta* **2007**, *52*, 4403.

(53) Baioni, A. P.; Vidotti, M.; Fiorito, P. A.; de Toressi, S. I. C. *J. Electroanal. Chem.* **2008**, *622*, 219.

(54) Ding, H.; Zhao, L.; Li, Y.; He, X. *Asian J. Chem.* **2008**, *20*, 2327.

(55) Jia, F.; Yu, C.; Gong, J.; Zhang, L. *J. Solid State Electrochem.* **2008**, *12*, 1567.

(56) Ojani, R.; Raoof, J.-B.; Fathi, S. *J. Solid State Electrochem.* **2009**, *13*, 837.

(57) Iveković, D.; Gajović, A.; Čeh, M.; Pihlar, B. *Electroanalysis* **2010**, *22*, 2202.

(58) Jin, E.; Lu, X.; Cui, L.; Chao, D.; Wang, C. *Electrochim. Acta* **2010**, *55*, 7230.

(59) Lisowska-Oleksiak, A.; Wilamowska, M.; Jasulaitiene, V. *Electrochim. Acta* **2011**, *56*, 3626.

(60) Tsai, T.-H.; Chen, T.-W.; Chen, S.-M. *Int. J. Electrochem. Sci.* **2011**, *6*, 4628.

(61) Yang, H.; Yuan, R.; Chai, Y.; Su, H.; Zhuo, Y.; Jiang, W.; Song, Z. *Electrochim. Acta* **2011**, *56*, 1973.

(62) Chen, L.; Wang, X.; Zhang, X.; Zhang, H. *J. Mater. Chem.* **2012**, *22*, 22090.

(63) Chen, S.-M.; Wang, C.-H.; Lin, K.-C. *Int. J. Electrochem. Sci.* **2012**, *7*, 405.

(64) Iveković, D.; Trbić, H. V.; Peter, R.; Petravić, M.; Čeh, M.; Pihlar, B. *Electrochim. Acta* **2012**, *78*, 452.

(65) Jin, R.; Li, L.; Lian, Y.; Xu, X.; Zhao, F. *Anal. Methods* **2012**, *4*, 2704.

(66) Mao, H.; Song, J.; Zhang, Q.; Liu, D.; Gong, N.; Li, Y.; Wu, Q.; Verpoort, F.; Song, X.-M. *Nanotechnology* **2013**, *24*.

(67) Doroftei, F.; Pinteala, T.; Arvinte, A. *Microchimica Acta* **2014**, *181*, 111.

(68) Mendes Castro Junior, J. G.; Mota Ferreira, G. M.; de Oliveira, F. G.; Damos, F. S.; Silva Luz, R. d. C. *J. Electroanal. Chem.* **2014**, *732*, 93.

(69) Gong, K. *J. Colloid Interface Sci.* **2015**, *449*, 80.

(70) Jomma, E. Y.; Bao, N.; Ding, S.-N. *Curr. Anal. Chem.* **2016**, *12*, 512.

(71) Karpova, E.; Karyakina, E. E.; Karyakin, A. A. *RSC Adv.* **2016**, *6*, 103328.

(72) Santos, D. M. F.; Saturnino, P. G.; Lobo, R. F. M.; Sequeira, C. A. C. *J. Power Sources* **2012**, *208*, 131.

(73) Shaegh, S. A. M.; Nguyen, N. T.; Ehteshami, S. M. M.; Chan, S. H. *Energy Environ. Sci.* **2012**, *5*, 8225.

(74) Yamada, Y.; Yoneda, M.; Fukuzumi, S. *Chem.–Eur. J.* **2013**, *19*, 11733.

(75) Yamada, Y.; Yoneda, M.; Fukuzumi, S. *Inorg. Chem.* **2014**, *53*, 1272.

(76) Raman, R. K.; Shukla, A. K. *J. Appl. Electrochem.* **2005**, *35*, 1157.

(77) Yamada, Y.; Yoshida, S.; Honda, T.; Fukuzumi, S. *Energy Environ. Sci.* **2011**, *4*, 2822.

(78) Mahesh, K.; Balaji, R.; Dhathathreyan, K. S. *Ionics* **2015**, *21*, 2603.

(79) Hernandez, J.; Solla-Gullon, J.; Herrero, E.; Feliu, J. M.; Aldaz, A. *J. Nanosci. Nanotechnol.* **2009**, *9*, 2256.

(80) Yang, X.; Ouyang, Y.; Wu, F.; Hu, Y.; Ji, Y.; Wu, Z. *Sens. Actuators, B* **2017**, *238*, 40.

(81) Tian, Y. M.; Huang, J. C.; Gao, Y.; Cao, D. X.; Wang, G. L. *J. Solid State Electrochem.* **2012**, *16*, 1901.

(82) Amirfakhri, S. J.; Pascone, P. A.; Meunier, J. L.; Berk, D. *J. Catal.* **2015**, *323*, 55.

(83) Zhang, R. Z.; Chen, W. *Biosens. Bioelectron.* **2017**, *89*, 249.

(84) Ernst, A. Z.; Zoladek, S.; Wiaderek, K.; Cox, J. A.; Kolary-Zurowska, A.; Miecznikowski, K.; Kulesza, P. J. *Electrochim. Acta* **2008**, *53*, 3924.

(85) Hamidi, H.; Shams, E.; Yadollahi, B.; Esfahani, F. K. *Electrochim. Acta* **2009**, *54*, 3495.

(86) Wang, C.; Hua, Y.; Tong, Y. *Electrochim. Acta* **2010**, *55*, 6755.

(87) Liu, J. Y.; Cheng, L.; Dong, S. J. *Electroanalysis* **2002**, *14*, 569.

(88) Martel, D.; Kuhn, A. *Electrochim. Acta* **2000**, *45*, 1829.

(89) Khoshro, H.; Zare, H. R.; Vafazadeh, R. *Chin. J. Catal.* **2014**, *35*, 247.

(90) Bagheri, H.; Ranjbari, E.; Amiri-Aref, M.; Hajian, A.; Ardakani, Y. H.; Amidi, S. *Biosens. Bioelectron.* **2016**, *85*, 814.